

# Forming Simulation of Thermoplastic Pre-Impregnated Textile Composite

Masato Nishi, Tetsushi Kaburagi, Masashi Kurose, Tei Hirashima, Tetsusei Kurasiki

**Abstract**—The process of thermoforming a carbon fiber reinforced thermoplastic (CFRTP) has increased its presence in the automotive industry for its wide applicability to the mass production car. A non-isothermal forming for CFRTP can shorten its cycle time to less than 1 minute. In this paper, the textile reinforcement FE model which the authors proposed in a previous work is extended to the CFRTP model for non-isothermal forming simulation. The effect of thermoplastic is given by adding shell elements which consider thermal effect to the textile reinforcement model. By applying Reuss model to the stress calculation of thermoplastic, the proposed model can accurately predict in-plane shear behavior, which is the key deformation mode during forming, in the range of the process temperature. Using the proposed model, thermoforming simulation was conducted and the results are in good agreement with the experimental results.

**Keywords**—Carbon fiber reinforced thermoplastic (CFRTP), Finite element analysis (FEA), Pre-impregnated textile composite, Non-isothermal forming.

## I. INTRODUCTION

THE increasing requirement for crash safety with weight reduction in the automotive industry has gradually expanded the use of carbon fiber reinforced plastic (CFRP) [1]. One of the reasons for the expansion is that the development of resin transfer molding (RTM) [2] has reduced its cycle time to less than 10 minutes. However, further shortening is required in order to be applied to the mass production of cars since the production cycle time needs to be less than 1 minute. Therefore thermoforming process of a carbon fiber reinforced thermoplastic (CFRTP) has increased its presence in the industry since it is a faster manufacturing process than RTM process which needs a long curing stage.

The first stage in the thermoforming process for CFRTP is the production of the pre-consolidated laminate. The thermoplastic resin pre-impregnated (pre-preg) sheets are stacked in the required orientation and are consolidated by a hot press. The isothermal process provides a high quality part but the cycle time is compromised due to the heating and cooling

times of the tools. In contrast, the non-isothermal process has a shorter cycle time. In this process, the pre-consolidated laminate is heated to forming temperature usually separately in an oven. The heated laminate is rapidly transferred to a forming tool. During forming the laminate is cooled by the contact with the tool and pressure can be removed after the temperature of the laminate has reduced to below the thermoplastic resin recrystallization level. Therefore the non-isothermal process requires no heating and cooling times. Consequently the cycle time of the non-isothermal process can be in the range of 1 minute [3].

Finite element analysis (FEA) as an alternative approach for experimental study is effective in designing fiber reinforced plastic products because there are many design parameters such as fiber type, resin type, morphology of fiber, volume fraction of fiber, fiber orientation, etc. Forming simulation is especially important because the performance of the final composite part strongly depends on changes in fiber orientation during the forming process. Sharma et al. [4] and Skordos et al. [5] proposed a discrete model that combines truss elements to represent uncoupled tension and shear properties of textile reinforcement. Aimene et al. [6] developed an anisotropic hyperelastic material model which independently calculates tension in the direction of warp and weft and in-plane shear for simulating the strong anisotropic behavior of textile reinforcement. These models ignore bending stiffness as it is significantly low compared to tensile stiffness. Notwithstanding bending stiffness plays a very important role in the prediction of wrinkles. In our previous work, a textile reinforcement model for FEA which can consider out-of-plane bending stiffness as well as in-plane anisotropic properties was proposed in order to predict the wrinkling [7]. Furthermore a micromechanical model that introduces a stress component due to yarn rotational friction is adapted to the proposed model to express the in-plane shear behavior that depends on the tensions in the yarns [8].

Thermoforming simulation for thermoplastic pre-pregs is more complex than the simulation for textile reinforcement because the material shows temperature and rate dependent behavior as well as anisotropic and nonlinear behavior. Wang et al. [9] and Haanappel et al. [10] proposed temperature and strain rate dependent friction models which can predict accurate slippage behavior but both material models were the anisotropic hyperelastic and viscous combined models. Both material models were generated by adding a viscosity model to a hyperelastic model in order to present the strain rate effect. If the volume fraction of fiber (Vf) of the pre-preg is changed, it is necessary to adjust the material parameters again to fit the

M. Nishi is with the Engineering Technology Division, JSOL Corporation, Tokyo, 104-0053, Japan (phone: +81-3-5859-6020, fax: +81-3-5859-6035, e-mail:nishi.masato@jsol.co.jp).

T. Kaburagi is with Gunma Industrial Technology Center, Gunma, 373-0019, Japan (e-mail: kaburagi-t@pref.gunma.lg.jp).

M. Kurose is with the Department of Mechanical Engineering, Gunma National College of Technology, Gunma, 371-8530, Japan (e-mail: kurose@mech.gunma-ct.ac.jp).

T. Hirashima is with the Engineering Technology Division, JSOL Corporation, Osaka, 550-0001, Japan (e-mail: hirashima.tei@jsol.co.jp).

T. Kurasiki is with the Department of Management of Industry and Technology, Osaka University, Osaka, 565-0871, Japan (e-mail: kurasiki@mit.eng.osaka-u.ac.jp).

experimental material behavior. Chen et al, [11] also proposed a model for a textile thermoplastic pre-preg forming simulation which considers the influence of the strain rate by adding a viscosity to the anisotropic hyperelastic model. This model as a parallel system of textile and resin calculates pre-preg stress from the properties of its fiber and thermoplastic using the micromechanical strain energy approach. Again, it ignores the bending mechanism. Moreover, these models [9]-[11] focused on isothermal forming simulation thus they did not consider the change in the temperature and material properties during forming. Non-isothermal forming has a limited design window because of the rapidly cooling pre-consolidated laminate and the decreasing formability which is caused by contact with the tool. So the temperature condition during forming should be carefully designed. Thus it is very important to simulate temperature change within the laminates and change in material properties due to temperature change.

The primary focus of this paper is on FE modeling and simulations performed to capture the forming behavior of a textile thermoplastic pre-preg. The possibility of extending the textile reinforcement model in the previous study [7], [8] to the thermoplastic pre-preg model for non-isothermal forming simulation is investigated. First, an FE model which considers the temperature dependent material behavior of the laminate is described. This model represents the stress of the textile and thermoplastic in a parallel system and by applying Ruess model to the stress calculation of thermoplastic enables the ability to predict temperature dependent in-plane shear behavior which is the key deformation mode during the forming of a textile composite [12]. Second, the temperature dependent in-planes shear behavior is verified by means of comparison to the results of bias-extension tests at the different temperatures. Finally, to assess the capability of the FE model, thermoforming simulations are conducted. The results of the sensitivity study using the proposed model pointed out that considering the effect of the temperature is important to accurately predict deformations during non-isothermal forming, and the comparison between the simulations and the experiments shows good agreement.

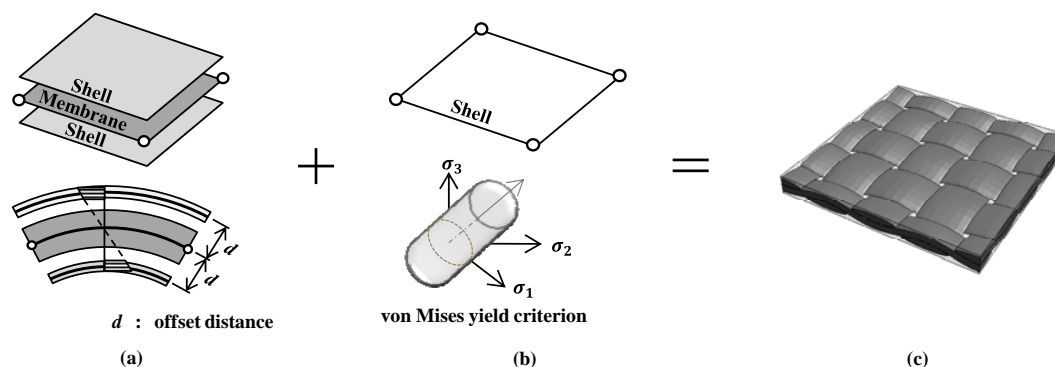


Fig. 1 Modeling schematic of textile thermoplastic pre-preg, (a) textile reinforcement model, (b) thermoplastic model and (c) pre-preg model

## II. CONSTITUTIVE MODELING

### A. Modelling Schematic

In this section, the development of the FE model of a textile thermoplastic pre-preg for non-isothermal forming is described. A forming simulation for non-isothermal process should be performed as a thermal-mechanical coupling analysis because the pre-preg temperature dramatically drops at and around the contact point with the tool and the material shows significant temperature dependent behavior. The objective is to extend the textile reinforcement model proposed in [7], [8] to the thermoplastic pre-preg model. The pre-preg consists of fibers in a textile structure embedded in a thermoplastic resin. Fig. 1 shows the schematic of the pre-preg model for non-isothermal forming simulation. The pre-preg model is assumed to be composed of anisotropic nonlinear textile reinforcement and temperature dependent isotropic elasto-plastic thermoplastic resin. In order to add the effect of thermoplastic resin to the textile reinforcement model, additional shell elements are placed around the textile membrane. Elements for the textile model and the thermoplastic model undergo the same displacement as they are represented in a parallel system. However the strain of the thermoplastic is calculated by introducing Ruess model [13] as described later.

The stress of the pre-preg is given as:

$$\sigma_{ij} = \sigma_{ij}^f + \sigma_{ij}^m \quad (1)$$

where  $\sigma_{ij}^f$  is the textile stress contribution and  $\sigma_{ij}^m$  is the thermoplastic stress contribution. These contributions are solved separately.

### B. Micromechanical Model for Textile Reinforcement

The mechanical behavior of the textile reinforcement is complex due to the intricate interactions of the yarns and fibers. The tensile stiffness in yarn direction is much higher than the others and shear response is highly nonlinear as shown in Fig. 2 [7]. Moreover bending stiffness differs depending on the direction of the yarn. It is not a continuous material so bending stiffness cannot be deduced from in-plane properties.

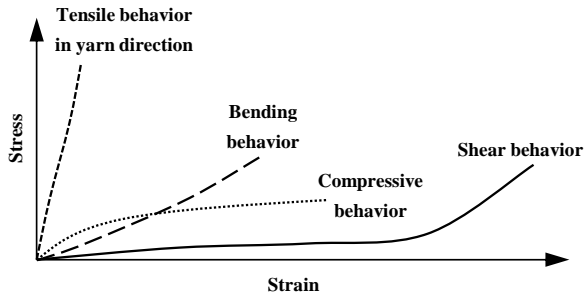


Fig. 2 Mechanical behavior of textile reinforcement

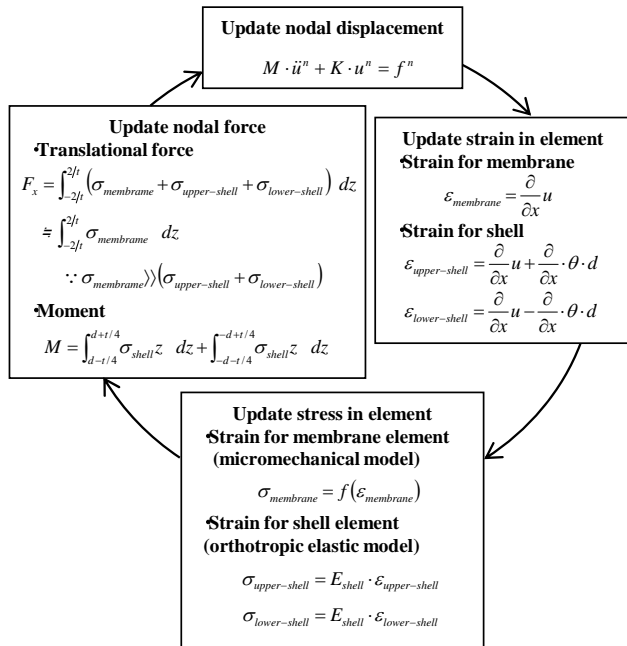


Fig. 3 Calculation loop in proposed textile reinforcement model [8]

Shell elements are usually used in metal forming simulation. The out-of-plane bending stiffness of a continuous material such as metal can be directly deduced from in-plane properties. However, the results of the textile reinforcement simulation using shell elements shows that the derived bending stiffness is unrealistically high compared to the experimental bending stiffness. Notwithstanding more accurate simulation is achievable by considering bending stiffness in forming simulation, the bending stiffness has been ignored as it is significantly low compared to tensile stiffness. This improvement in accuracy is especially remarkable for wrinkling. We proposed the shell and membrane combined model in order to consider bending stiffness in our previous work [7], [8]. Fig. 1 (a) shows the composition of our proposed model. In-plane properties are described by the membrane element and the bending stiffness is represented by a set of elements which consists of two shell elements with the membrane element in between them. The shell reference surface is offset to enhance the effect of bending stiffness. This enables the shell elements to have a Young's modulus small enough not to affect the in-plane properties but large enough to

effect to bending stiffness. Fig. 3 shows the calculation loop in the textile model. It is assumed that the bending stiffness is independently free from any in-plane deformations. The effects of off-axis bending stiffness can be calculated by giving an orthotropic material formulation to the two shell elements.

Moreover, a micromechanical model proposed by Ivanov et al. [14] is adapted to the membrane element within our proposed shell and membrane combined model in order to describe the in-plane behavior. This textile reinforcement model can account for the trellising with reorientation of the yarns and their locking. Textile reinforcement consists of periodic architecture of yarns. This periodic architecture is called the representative volume cell (RVC). The RVC consists of undulated yarns arranged in a crisscross pattern as shown in Fig. 4. The parameters of this model are as follows: the yarn span  $s$ , the textile thickness  $t$ , the yarn width  $w$ , the yarn cross-sectional area  $S$ , and the elastic constants of the yarn defined as a transversely isotropic elastic material. The stress calculation of the micromechanical model that utilizes the RVC is explained below.

- 1) The in-plane rotation of yarns is calculated by using the deformation gradient tensor.
- 2) The strain tensor of the RVC is transformed from the RVC coordinate system to the yarn direction in order to determine the stress response of yarn.
- 3) The stress response of the yarns can be derived from the defined elastic constants of the yarn. The transverse Young's modulus of the yarns and the longitudinal shear modulus are reduced to zero before the shear locking here.
- 4) The stress tensor based on the yarn material coordinate system is transformed into that of the RVC coordinate system.

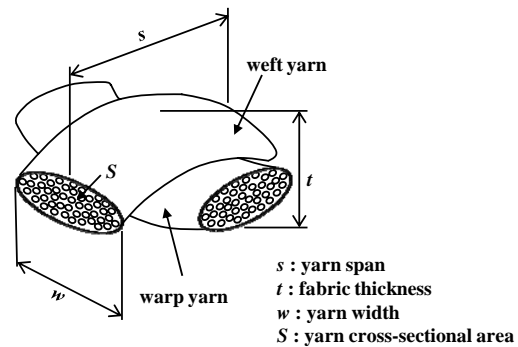


Fig. 4 Representative volume cell of micromechanical model [14]

### C. Effect of Thermoplastic Resin

The contribution of thermoplastic resin is added to the textile reinforcement. The thermoplastic material is an isotropic elasto-plastic model with von Mises yield criterion which considers thermal effects. The calculation of resin stress considers temperature dependent elastic properties, decreasing yield stress value for increasing temperature and nonlinear relation between yield stress and equivalent plastic strain. The contribution of the thermoplastic is most important for in-planeshear behavior especially before shear locking of the

textile reinforcement [15].

Stress response of the pre-preg is represented in a parallel system of textile reinforcement and thermoplastic resin where those stresses are separately calculated. The stress contribution of the thermoplastic in yarn direction, 0/90, is much less important than in 45/-45 direction since the stiffness of the yarn is much higher than the stiffness of the thermoplastic. Therefore the main purpose of the additive stress contribution of the thermoplastic on the textile is to describe their in-plane shear response of the pre-preg.

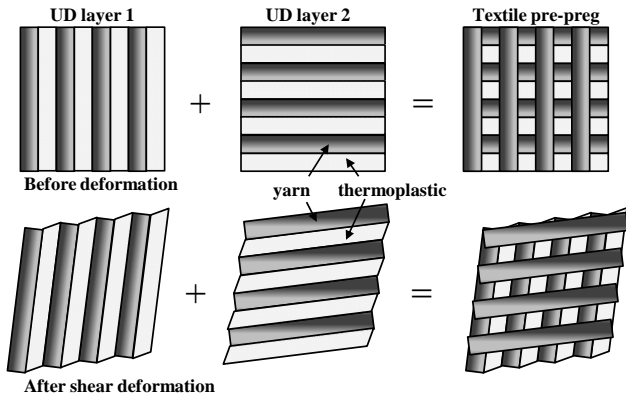


Fig. 5 Schematic illustration of textile as superposed two UD layers

To simplify the meso-scale material structure, the textile pre-preg is made up of two different superposed layers which consist of unidirectional fibers (UD layer) as shown in Fig. 5. The fiber direction of first layer is oriented initially at 90° with respect to the second layer. Each layer is deformed freely without any interaction. As a result of this simplified assumption, any effect of textile architecture becomes ignorable. Reuss model [13], which is developed from the assumption of equal stress in fiber and resin and is often used to predict the in-plane shear property of a UD material as an elementary micromechanical approach, can be adapted to the stress calculation of resin in each layer under in-plane shear deformation. The stress of the thermoplastic is calculated by:

$$\sigma_{ij}^m = f_m(\varepsilon_{ij}^m, T) \quad (2)$$

$$\varepsilon_{ij}^m = \frac{\varepsilon_{ij} - V_f \cdot \varepsilon_{ij}^f}{(1 - V_f)} \quad (3)$$

where  $f_m(\varepsilon_{ij}^m, T)$  is the stress response of the thermoplastic and is a function of  $\varepsilon_{ij}^m$ , thermoplastic strain, and  $T$ , temperature.  $\varepsilon_{ij}^m$  is calculated based on Reuss model.  $\varepsilon_{ij}$  is the macro strain of the pre-preg.  $V_f$  is the fiber volume fraction. Here, because the fiber stiffness is usually much higher than resin stiffness,  $\varepsilon_m$  can be approximated as:

$$\varepsilon_{ij}^m = \frac{\varepsilon_{ij}}{(1 - V_f)} \quad (4)$$

The in-plane shear stress component of the micromechanical

model for the textile reinforcement before shear locking is almost zero since the transverse Young's modulus of the yarns and the longitudinal shear modulus are reduced to zero as mentioned in Section II B. The stress contribution of the thermoplastic dominates the in-plane shear response before the shear locking stage in this parallel model of textile reinforcement and resin.

#### D. Heat Transfer Calculation between Pre-Preg and Tool

During the non-isothermal forming, the pre-preg blank experiences rapid temperature drop at and around the contact point with the tool. The material properties of the pre-preg are significantly changed by the temperature drop. Actually the surface without any contact loses heat to the environment by air convection and thermal radiation but the heat transfer to the tool due to contact is much greater. Therefore the effects of air convection and thermal radiation are ignored and only the heat transfer on the contact surface is considered in this study. An accurate heat transfer calculation between pre-preg and tool is essential to accurately simulate the deformation behavior of the pre-preg during the non-isothermal forming because of the significant effect the temperature gives to the material properties especially the in-plane shear property.

The contact heat transfer between the blank and tool on the contact surface can be obtained from:

$$\dot{q} = hA(T_p - T_t) \quad (5)$$

where  $A$  is the contact area between pre-preg and tool surfaces.  $T_p$  and  $T_t$  are the node temperatures of the pre-preg and tool at the contact point.  $h$  is the heat transfer conductance of the contact surface and is a function of the distance between the pre-preg and tool,  $L_{gap}$ .

$$h = h_{contact}, \text{ if } 0 \leq L_{gap} < L_{min} \quad (6)$$

$$h = \frac{k}{L_{gap}}, \text{ if } L_{min} \leq L_{gap} < L_{max} \quad (7)$$

$$h = 0, \text{ if } L_{max} \leq L_{gap} \quad (8)$$

### III. MODEL VALIDATION FOR IN-PLANE SHEAR BEHAVIOR

#### A. Bias-Extension Test

The textile thermoplastic pre-preg tested in this work is composed of plain weave carbon fiber fabric and polymethyl-methacrylate (PMMA) resin. PMMA is a thermoplastic polymer. The temperature of glass-liquid transition ( $T_g$ ) of PMMA is 108°C. Pre-consolidated laminate that has four pre-preg layers is produced by a hot press at a temperature above the melting point of PMMA.  $V_f$  of the laminate after pre-consolidation is 70% and the thickness of the laminate with 4 ply is 0.84mm on average.

A large in-plane shear deformation typically occurs during the forming of a textile laminate since the in-plane shear resistance is very low until the textile laminate reaches the shear locking angle. Thus accurately expressing the in-plane shear behavior of a textile laminate is very important for accurate forming simulation as mentioned before. A

bias-extension test is a popular approach to measure the shear property of a textile laminate. It is a tensile test performed on a rectangular specimen where the warp and weft yarns are oriented initially 45°/45° to the direction of applied tensile load. The specimen for a bias-extension test is divided into three regions which deform at different rates as shown in Fig. 6. If the yarns are considered inextensible and no intra-ply slip occurs within the specimen, the shear angle in zone A is always twice the angle in zone B while zone C remains undeformed. Under this kinematic assumption, the pure shear can be produced in zone A. Shear angle  $\gamma$  and shear force  $F_{sh}$  in zone A are calculated as follows [16]:

$$\gamma = \frac{\pi}{2} - 2 \cos^{-1} \left( \frac{D+d}{\sqrt{2}D} \right) \quad (9)$$

$$F_{sh}(\gamma) = \frac{F_c}{\cos \gamma} \left( \cos \left( \frac{\gamma}{2} \right) - \sin \left( \frac{\gamma}{2} \right) \right) - F_{sh} \left( \frac{\gamma}{2} \right) \quad (10)$$

where  $d$ ,  $D$  and  $F_c$  are the loading displacement, the length of pure shear zone and the load cell force, respectively. With (9) and (10), a shear angle versus shear force curve from the bias-extension test is obtained.

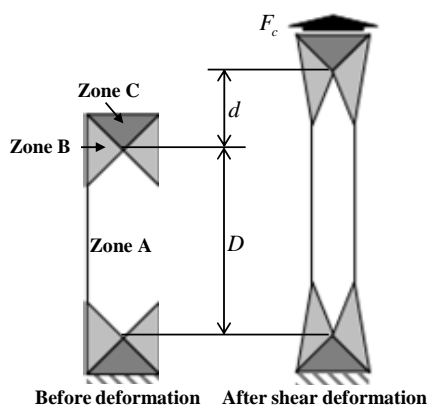


Fig. 6 Schematic representation of a bias-extension test

In this study, bias-extension tests were performed with an extension speed of 4mm/min at six different temperatures, 25°C, 50°C, 100°C, 150°C, 180°C and 200°C. A 150mm×25mm rectangular form cut out from pre-consolidated laminate is the specimen.

TABLE I  
MATERIAL PARAMETERS FOR TEXTILE MICROMECHANICAL MODEL

| Parameters for micromechanical model                 |          |
|--|----------|
| yarn span: $s$ (mm)                                  | 2.0      |
| textile thickness: $t$ (mm)                          | 0.24     |
| yarn width: $w$ (mm)                                 | 1.7      |
| yarn cross-sectional area: $S$ (mm <sup>2</sup> )    | 0.15     |
| longitudinal Young's modulus of yarn: $E_{11}$ (MPa) | 17,357.0 |
| transverse Young's modulus of yarn: $E_{12}$ (MPa)   | 11.0     |
| longitudinal shear modulus of yarn: $G_{12}$ (MPa)   | 1.0      |
| shear locking angle: $\theta_{lock}$ (°)             | 32.0     |

### B. Comparison between Model and Experiment

Simulations of the bias-extension tests are also performed at six different temperatures. Fig. 7 shows comparisons of load responses between experimental measurements and simulation results at respective temperatures.

From the experimental measurements (dot lines in Fig. 7), we can observe the influence of temperature on the in-plane shear response of the thermoplastic laminate. At temperatures under Tg, 25°C, 50°C and 100°C, the stress-strain relationship is similar to elasto-plastic behavior, and at about 30° shear angle, localized necking occurs. Furthermore, fracture of the laminates occurred at 32° and 46° shear angles at 25°C and 50°C, respectively. At the high temperatures over Tg, 150°C, 180°C and 200°C, the thermoplastic laminates produced a much smaller shear resistance than those of under Tg. The material shear stiffness increased as the shear angle increased. The stiffness tended to increase at around a 35° shear angle due to the shear locking. Fig. 8 shows the experimental specimens before and after shear deformation at 180°C. At temperatures higher than Tg, we observed squeeze flow of thermoplastic resin after the shear locking. At the same time, the jagged edge found after the bias-extension test revealed that the test had induced intra-ply slip between yarns as well as trellising after shear locking. In [17], the deformation resistance of the bias-extension test after shear locking becomes lower than that of the picture frame test since the intra-ply slip accommodates the imposed displacement in the bias-extension test. The bias-extension test results appear to be valid before it reaches the 35° shear locking angle. The experimental results at 180°C and 200°C were similar to each other. From these experimental results, the temperature dependent shear property has to be considered, especially for non-isothermal forming because the in-plane shear property strongly depends on temperature during the forming.

The simulations of the bias-extension tests have been done by general finite element solver LS-DYNA [18] with the proposed thermoplastic pre-preg model. To compare the results from the experiments and simulations correctly, specimens of the same dimensions as used in the experiments are used in the simulations. The dry textile reinforcement properties used for the calculations are taken from [7]. Table I shows material parameters which are used. The stress-strain relationships of PMMA under Tg, 25°C, 50°C and 100°C, used for the simulations are taken from CAMPUS database [19]. Those over Tg, 150°C, 180°C and 200°C are identified by fitting the experimental results since there is no database of stress-strain relationships over Tg.

The simulation responses are shown in Fig. 7 (solid lines), along with the experimental measurements. The difference between the simulation and experimental results after 20° of shear angle under Tg is presented. The reason for the difference is the mismatch in Poisson strains between the textile model and the thermoplastic model as shown in Fig. 9. The textile model tends to shrink under shear deformation, because its yarn scarcely stretches and its dominant deformation is a rotation between yarns at the cross over point. On the other hand, the

thermoplastic is calculated under the assumption that the volume remains constant in plastic deformation. Consequently, the conflict of the change in volume between the textile model and the thermoplastic model prevents the rotation of yarn in the micromechanical textile model. The absence of rotation leads to the generation of a tensile load in the yarn of the textile model, and results in the shear reaction force of the model increasing after the shear angle reaches 20°. However, we can see good agreements between the simulation and experimental results up to a 20° shear angle. Regarding the temperature range

over T<sub>g</sub>, a good correlation with the experimental force up to 35° after shear locking angle over T<sub>g</sub> is obtained by adjusting the properties of PMMA. As mentioned above, the bias-extension test results over T<sub>g</sub> are valid before it reaches 35° of the shear locking angle but are not valid after it reaches shear locking angle due to the intra-ply slip. Representing the shear behavior over T<sub>g</sub> in the model is much more important than that under T<sub>g</sub> because the thermoforming process for CFRTP is usually conducted over T<sub>g</sub>.

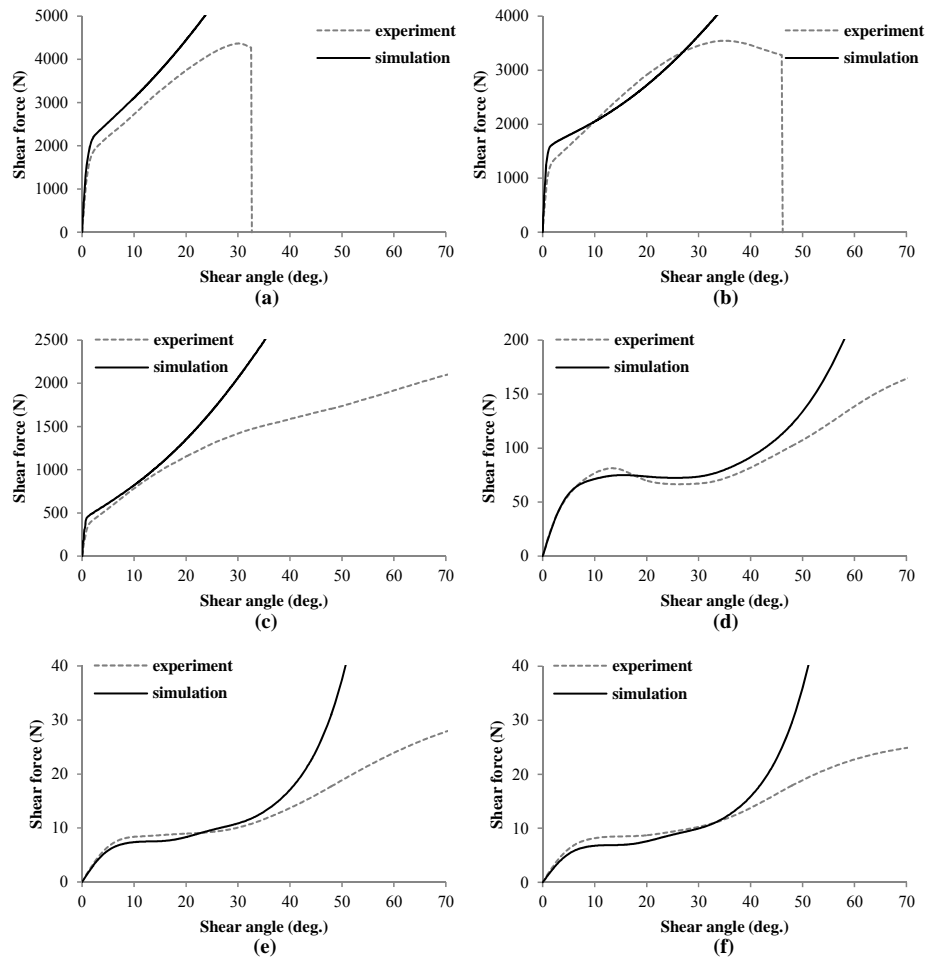


Fig. 7 Comparison of shear responses under bias-extension tests at (a) 25°C, (b) 50°C, (c) 100°C, (d) 150°C, (e) 180°C, and (f) 200°C

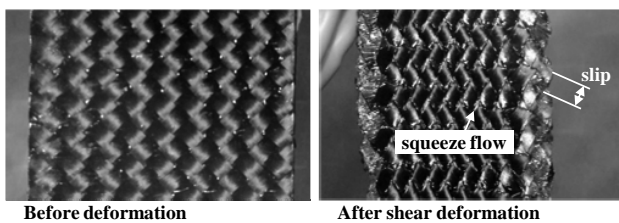


Fig. 8 Specimens of bias-extension tests at 180°C

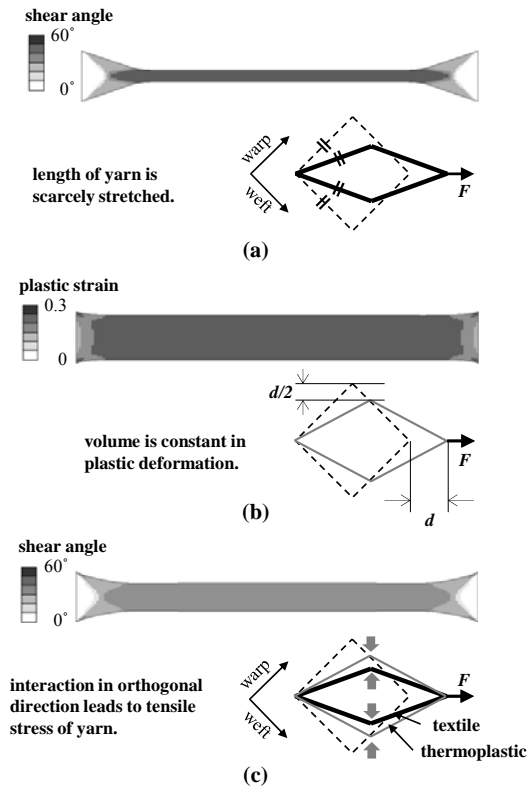


Fig. 9 Interaction between textile and thermoplastic model (a) textile model, (b) thermoplastic model and (c) pre-preg model

#### IV. THERMOFORMING SIMULATION

##### A. S-Rail Forming

Pre-consolidated laminates consist of four textile thermoplastic pre-preg layers. Simple laminates with  $[(0/90)]_4$  and  $[(45/-45)]_4$  lay-ups were tested experimentally in order to assess the capability of the proposed FE model. The blank was cut in square form, 250mm×250mm. An S-rail problem was adopted for its simplified shape of automotive side member. Forming experiments were performed with a non-heated steel tool at room temperature. First, the pre-consolidated laminate was heated to forming temperature separately in an oven. Then it was rapidly transferred to a forming tool and formed by the

downward movement of the punch at a speed of 20mm/s. The temperature of the laminate, which was measured just before the forming process, was uniformly distributed over the majority of the surface area. Its average temperature was 185°C which were measured by thermography.

TABLE II  
THERMAL PARAMETERS FOR THERMAL ANALYSIS

| Parameters for thermal analysis   |        |
|---|--------|
| thermal conductivity: $k$ (mJ/(mm <sup>3</sup> ·s·K))                     | 0.0241 |
| heat transfer conductance: $h_{contact}$ (mJ/(mm <sup>2</sup> ·s·K))      | 3.0    |
| minimum gap: $L_{min}$ (mm)   | 0.01   |
| maximum gap: $L_{max}$ (mm)   | 0.4    |
| in-plane thermal conductivity of pre-preg: $K_{11}, K_{22}$ (mJ/(mm·s·K)) | 3.4135 |
| out-of-plane thermal conductivity of pre-preg: $K_{33}$ (mJ/(mm·s·K))     | 0.6825 |
| heat capacity of pre-preg: $HC$ (mJ/(g·K))                                | 1106.0 |
| thermal conductivity: $k$ (mJ/(mm <sup>3</sup> ·s·K))                     | 0.0241 |

Simulations are also performed by two different approaches to investigate the effect of the change in the temperature during the forming. One is non-isothermal simulation by thermal-mechanical coupling analysis which can consider the change in the temperature during forming. The other is isothermal simulation by simple mechanical analysis under the assumption of a constant temperature during the forming process. For the thermal-mechanical coupling analysis, the mechanical analysis is solved by explicit method and the thermal analysis is solved by implicit method. The heat transfer conductance between pre-preg laminate and tool is determined by reference to the database of the commercial plastics injection molding software Molex3D [20]. Thermal conductivity of the pre-preg laminate is calculated by Eshelby-based semi-analytical mean-field homogenization approaches in Digimat software [21]. Table II shows the thermal parameters which are used in this work. The initial temperature for the blank and steel tools is set at 185°C and room temperature is set at 25°C. Fig. 10 shows the simulation model. The die and punch are modeled as rigid bodies. Each pre-preg layer is meshed separately by the proposed model. Pre-preg layers are constrained to prevent slippage between the neighboring layers because there was no slippage observed in the experiments.

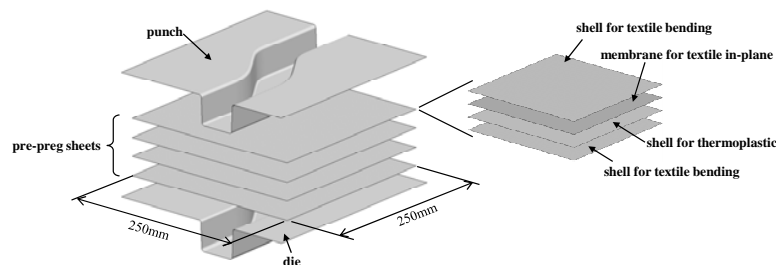


Fig. 10 S-rail forming simulation model for multi-layers

### B. Comparison between Experiment and Simulation

Fig. 11 shows the comparisons of the outlines between the experiments and each simulation, non-isothermal simulation and iso-thermal simulation. The outlines simulated by the non-isothermal simulations show good agreement with the experimental measurements for both laminates with  $[(0/90)]_4$  and  $[(45/-45)]_4$  lay-ups. On the other hand, the outlines simulated by the isothermal simulations are different from the experimental measurements for both lay-ups. Fig. 12 shows the comparison of the shear angle in the side wall, between experiment and simulations for the  $[(0/90)]_4$  lay-up. The reason for the larger draw-in in the isothermal simulation is that the shear deformation in the side wall, especially near the corner of punch is larger than the experiment and the non-isothermal

simulation:  $71^\circ$  for the experiment,  $61^\circ$  for the isothermal simulation and  $71^\circ$  for the non-isothermal simulation respectively.

Fig. 13 shows the distributions of the temperature in the laminate of the  $[(0/90)]_4$  lay-up in the non-isothermal simulation. It describes that the temperature of the laminate in the side wall near the corner of punch drops during the forming process. This drop is due to contact with the punch. The shear resistance is dramatically increased by the decreased temperature. Consequently, the shear deformation in the non-isothermal simulation is smaller than in isothermal simulation which assumes the constant temperature. These simulation results demonstrated that formability is significantly changing throughout the non-isothermal forming.

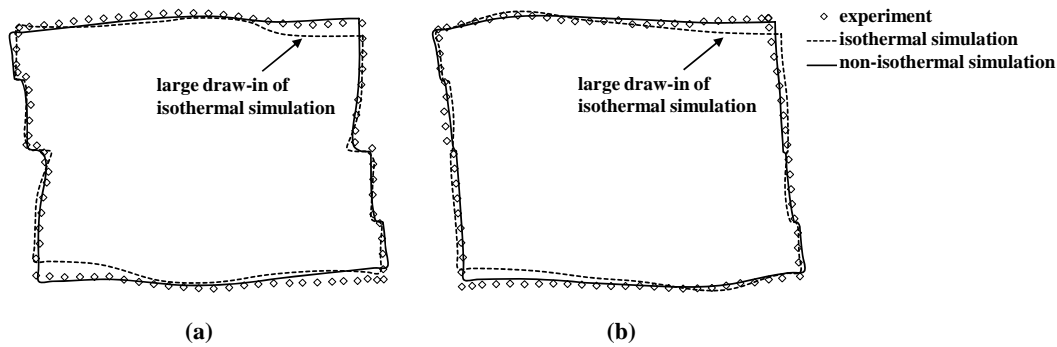


Fig. 11 Comparison of final outlines between experiments and simulations of (a)  $[(0/90)]_4$  and (b)  $[(45/-45)]_4$  lay-ups

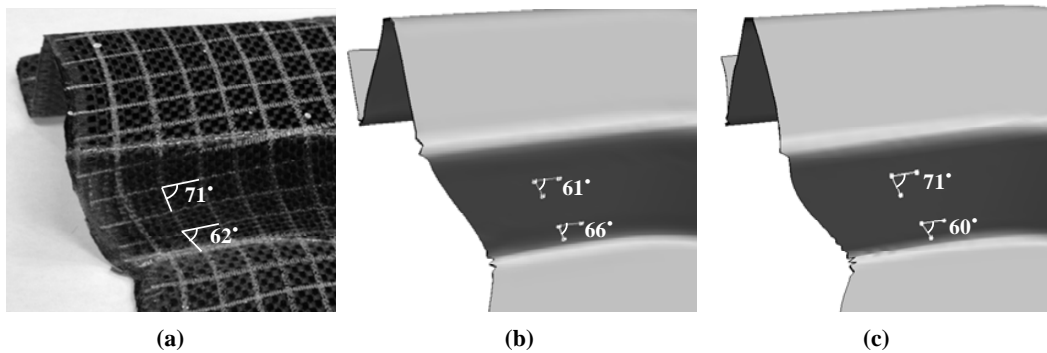


Fig. 12 Comparison of shear angle of  $[(0/90)]_4$  lay-ups between (a) experiment and (b) isothermal simulation, and (c) non-isothermal simulation

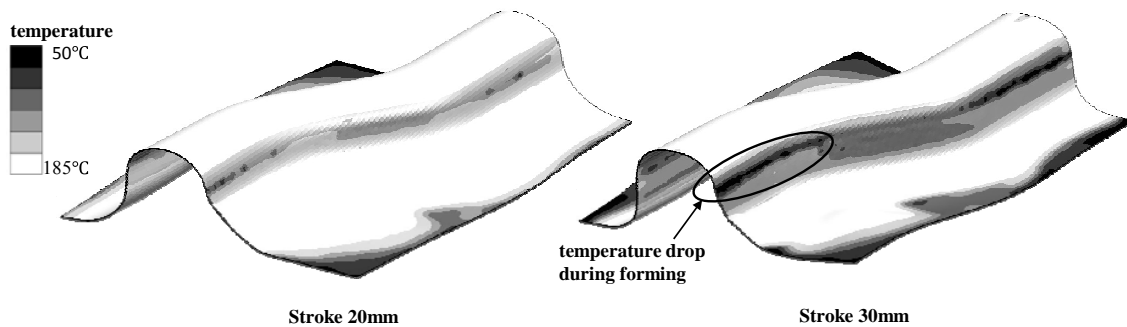


Fig. 13 Temperature distribution during non-isothermal forming simulation



## V. CONCLUSION

An FE model for non-isothermal forming of a textile thermoplastic pre-preg was proposed in this study. The proposed model can accurately predict the experimental in-plane shear response of the bias-extension by applying Ruess model to the stress calculation of thermoplastic. It is possible to predict the material behavior of the pre-preg from the thermoplastic properties and Vf. This will be helpful in textile pre-preg material characterization when it is difficult to measure experimentally, e.g. under high temperature. This model also has the capability to consider the change in temperature during forming and the temperature dependent material property by thermal-mechanical coupling analysis. The model was verified by comparing the in-plane shear response between the result from the simulations of a bias-extension test and experimental measurements. A good correlation between the simulation result and the experimental measurements was confirmed. For the effect of the temperature dependent material behavior on the forming simulation results, S-rail forming simulations of pre-preg laminate were conducted as well. Results of this sensitivity study pointed out that considering the effect of the temperature is important to accurately predict deformation during non-isothermal forming. The deformations predicted by the proposed model agreed well with experimental results.

It is important to predict, by simulation, the formability of the pre-preg composite such as the final shape of product, fiber orientation of the different layers and possible wrinkles and the temperature condition during forming. Notwithstanding the fact that the non-isothermal forming process has a limited time and temperature design window, it is attractive to the mass production cars due to its shorter cycle time. The proposed FE model in this study will be helpful to understand pre-preg behavior including change in temperature during non-isothermal forming. This plays a part in optimization of the non-isothermal forming process and reducing its product development time.

## ACKNOWLEDGMENT

The experiments of non-isothermal forming were conducted at Asano Corporation and were guided by Hitoshi Nakamura. The good support is gratefully acknowledged. The work was funded by Strategic Foundational Technology Improvement Support Operation 2012-2014. Furthermore authors would like to thank Prof. Masaru Zako at Osaka University for all helpful discussion of the work.

## REFERENCES

- [1] L. Ulich, P. Fairley, "Carbon car [2013 Tech To Watch]", *IEEE Spect.*, vol. 50, pp.30-31, 2013.
- [2] C.D Rudd, A.C Long, K N Kendall, C. Mangin, *Liquid molding technologies*, CRC Press, Woodhead Pub.: Cambridge, UK, 1997, pp.12-27.
- [3] A.C. Long, *Composite forming technologies*, CRC Press, Woodhead Pub.: Cambridge, UK, 2007, pp.256-276.
- [4] S.B. Sharma, M.P.F. Sutcliffe, "A simplified finite element model for draping of woven material", *Compos. Part A: Appl. Sci. Manuf.*, vol.35, pp.637-643, 2004.
- [5] A.A. Skordos, C.M. Aceves, M.P.F. Sutcliffe, "A simplified rate dependent model of forming and wrinkling of pre-impregnated woven composites", *Compos. Part A: Appl. Sci. Manuf.*, vol.38, pp.1318-1330, 2007.
- [6] Y. Aïmene, B. Hagege, F. Sidoroff, E. Vidal-Salle, P. Boisse, S. Dridi, "Hyperelastic approach for composite reinforcement forming simulations", *Int. J. Mater. Form.*, vol.1, pp.811-814, 2011.
- [7] M. Nishi, T. Hirashima, "Approach for dry textile composite forming simulation", in *Proc.19<sup>th</sup> Int. Conf. Compos. Mat.*, Canada, 2013.
- [8] M. Nishi, T. Hirashima, T. Kurashiki, "Textile composite reinforcement forming analysis considering out-of-plane bending stiffness and tension dependent in-plane shear behavior", in *Proc. 16<sup>th</sup> Eur. Conf. Compos. Mat.*, Spain, 2014.
- [9] P. Wang, N. Hamila, P. Boisse, "Thermoforming simulation of multilayer composites with continuous fibres and thermoplastic matrix", *Compos. Part B: Eng.*, vol.52, pp.127-136, 2013.
- [10] S.P. Haanappel, R.H.W. ten Thije, U. Sachsa, B. Rietman, R. Akkerman, "Formability analyses of uni-directional and textile reinforced thermoplastics", *Compos. Part A: Appl. Sci. Manuf.*, vol.56, pp.80-92, 2014.
- [11] Q. Chen, P. Boisse, C.H. Park, A. Saouab, J. Breard, "Intra/inter-ply shear behaviors of continuous fiber reinforced thermoplastic composites in thermoforming processes", *Compos. Struct.*, vol.93, pp.1692-1703, 2011.
- [12] P. Boisse, B. Zouari, J.L. Daniel, "Importance of in-plane shear rigidity in finite element analyses of woven fabric composite preforming", *Compos. Part A: Appl. Sci. Manuf.*, vol.37, pp.2201-2212, 2006.
- [13] D. Hull, T.W. Clyne, *An Introduction to Composite Materials*, Cambridge University Press: New York, 1996, pp.60-77.
- [14] I. Ivanov, A. Tabiei, "Loosely woven fabric model with viscoelastic crimped fibres for ballistic impact simulations", *Int. J. Numer. Methods Eng.*, vol.61, pp.1565-1583, 2004.
- [15] P. Harrison, M.J. Clifford, A.C. Long, C.D. Rudd, "A constituent-based predictive approach to modelling the rheology of viscous textile composites", *Compos. Part A: Appl. Sci. Manuf.*, vol.35, pp.915-931, 2004.
- [16] J. Launay, G. Hivet, A.V. Duong, P. Boisse, "Experimental analysis of the influence of tensions on in plane shear behavior of woven composite reinforcements", *Compos. Sci. Technol.*, vol.68, pp.506-515, 2008.
- [17] P. Harrison, M.J. Clifford, A.C. Long, "Shear characterisation of viscous woven textile composites: a comparison between picture frame and bias extension experiments", *Compos. Sci. Technol.*, vol.64, pp.1453-1465, 2004.
- [18] J.O. Hallquist, *LS-DYNA Theory Manual*, ISBN 0-9778540-0-0, 2006.
- [19] CAMPUS, Available: <http://www.campusplastics.com/campus>
- [20] Molex3D, Available: <http://www.moldex3d.com/en/>
- [21] Digimat, Available: <http://www.e-xstream.com/en/index.html>.